Natural Resources for Human Health
eISSN: 2583-1194

Original Research

Received 26 May 2026
Revised 22 June 2026
Accepted 20 July 2026

Natural Resources for Human Health 2026, Vol. 6 (7s): 422–433

KEYWORDS:
Kaempferol; Syzygium myrtifolium; biofilm inhibition; Enterococcus faecalis; Staphylococcus aureus; endodontic infection.

Kaempferol from Syzygium myrtifolium Leaves: Isolation, Structural Elucidation, and Antibiofilm Activity Against Pathogenic Root Canal Bacteria

Risyandi Anwar1*, Steffi Triany Arnov2

[1]Herbal Medicine Research, Department of Pediatric Dentistry, Faculty of Dental Medicine, Universitas Muhammadiyah Semarang, Semarang 50272, Indonesia
[2]Department of Periodontia, Faculty of Dental Medicine, Universitas Muhammadiyah Semarang, Semarang 50272, Indonesia
*Corresponding author: Risyandi Anwar; Herbal Medicine Research, Department of Pediatric Dentistry, Faculty of Dental Medicine, Universitas Muhammadiyah Semarang, Jl. Kedungmundu No. 18, Semarang 50272, Indonesia. E-mail: drg.risyandi@unimus.ac.id

ABSTRACT: Persistent root canal infection remains a major challenge in endodontic therapy, largely attributable to bacterial biofilms formed by Enterococcus faecalis and Staphylococcus aureus that resist conventional irrigants such as sodium hypochlorite. Plant-derived flavonoids, including kaempferol, have shown promising antibiofilm and antibacterial properties, yet the isolation of kaempferol specifically from Syzygium myrtifolium Walp. (red shoot) leaves and its inhibitory activity against these endodontic pathogens have not been previously reported. This study aimed to isolate and structurally characterize kaempferol from S. myrtifolium leaves and to evaluate its inhibitory effect on mixed-species biofilm formation by E. faecalis and S. aureus. The dried leaf powder was macerated in 96% ethanol, partitioned sequentially with n-hexane and ethyl acetate, and the ethyl acetate fraction was subjected to gravity column chromatography guided by thin-layer chromatography. A pure isolate was obtained and characterized using UV, IR, HR-ESI-TOF-MS, and one-dimensional NMR spectroscopy (1H, 13C, DEPT-135). Spectroscopic data (molecular formula C15H10O6; m/z 287.0556 [M+H]+) together with comparison to reference NMR data confirmed the isolate as kaempferol (3,4',5,7-tetrahydroxyflavone). In a crystal violet biofilm assay, kaempferol produced concentration-dependent inhibition of mixed-species E. faecalis–S. aureus biofilm formation, with the 5 µg/mL concentration showing antibiofilm efficacy statistically comparable to 0.2% chlorhexidine at both 24 h and 48 h ($p > 0.05$). These findings support kaempferol from S. myrtifolium leaves as a promising natural antibiofilm candidate against clinically relevant endodontic pathogens and provide a structural basis for its further development as an adjunctive agent in root canal disinfection

1. INTRODUCTION

Pulpal and periapical diseases remain among the most common oral health problems worldwide. The global prevalence of apical periodontitis reaches approximately 52% at the individual level and 5% at the tooth level, indicating that more than half of the world's adult population carries at least one tooth affected by this condition (Tibúrcio-Machado et al., 2021). In Indonesia, national data from the 2018 Basic Health Research (Riset Kesehatan Dasar/Riskesdas) survey reported that 57.6% of the population experienced oral and dental health problems, with dental abscess—including periapical abscess arising from pulpal infection—accounting for 14% of the most frequently encountered dental conditions (Kemenkes RI, 2018). These figures

highlight that pulpal and periapical infections, most of which originate from untreated dental caries progressing to pulp necrosis, constitute a substantial and largely preventable burden of oral disease both globally and within the Indonesian population.

Root canal infections are polymicrobial diseases in which microorganisms predominantly persist as structured biofilm communities within the root canal system. Compared with planktonic bacteria, biofilm-associated microorganisms exhibit altered physiological characteristics and are embedded within an extracellular polymeric matrix that enhances their tolerance to environmental stress and antimicrobial agents. The anatomical complexity of the root canal system and the multispecies nature of endodontic biofilms further complicate microbial eradication, making biofilm persistence a major biological challenge in the prevention of post-treatment disease and endodontic treatment failure (Siqueira & Rôças, 2022; Neelakantan et al., 2017).

Among the microorganisms associated with persistent intraradicular infection, *Enterococcus faecalis* has received particular attention because of its capacity to survive under nutrient limitation and other adverse environmental conditions, penetrate dentinal tubules, and establish biofilms on root canal-related surfaces (Alghamdi & Shakir, 2020). Importantly, a systematic review involving 972 teeth demonstrated that *E. faecalis* was significantly more frequently detected in persistent intraradicular infections than in untreated primary infections, with an odds ratio of 7.247 (95% CI, 4.039–13.002) (Zhang et al., 2015). These characteristics highlight the ability of *E. faecalis* to persist despite conventional endodontic disinfection and support its relevance as a target microorganism in the development of improved antibiofilm strategies.

The complexity of endodontic biofilms, however, cannot be attributed to a single bacterial species. *Staphylococcus aureus*, another Gram-positive facultative bacterium, has demonstrated the capacity to form biofilms on gutta-percha and to participate in multispecies endodontic-like biofilm communities (Noiri et al., 2004; Abusrewil et al., 2020). Experimental studies have confirmed biofilm formation by both *E. faecalis* and *S. aureus* on gutta-percha surfaces, while multispecies endodontic biofilm models have demonstrated that both species can successfully establish within dentin-associated microbial communities. Therefore, simultaneous consideration of *E. faecalis* and *S. aureus* may provide a more relevant experimental approach for evaluating novel antibiofilm agents intended for endodontic applications.

The persistence and complexity of endodontic biofilms have consequently stimulated interest in alternative antimicrobial strategies, particularly those targeting biofilm formation rather than bacterial viability alone. In this context, plant-derived secondary metabolites have emerged as promising sources of bioactive compounds because several phenolic and flavonoid constituents exhibit antimicrobial and antibiofilm properties. *Syzygium myrtifolium* Walp., commonly known as red shoot or pucuk merah, is particularly interesting because its leaves contain diverse secondary metabolites, including flavonoids and phenolic compounds, and its extracts have demonstrated antibacterial activity against several bacterial species, including *S. aureus* (Wu et al., 2017; Ahmad et al., 2022).

Taken together, the established role of biofilms in persistent endodontic infection, the documented ability of *E. faecalis* and *S. aureus* to participate in root canal-associated biofilms, and the emerging antibiofilm potential of plant-derived flavonoids provide a compelling rationale for investigating a flavonoid isolate from *S. myrtifolium* leaves as a candidate antibiofilm compound. Evidence on the activity of this isolate against both *E. faecalis* and *S. aureus* in an endodontic context remains limited. Therefore, evaluating the antibiofilm activity of the *S. myrtifolium* isolate against these two clinically relevant microorganisms may provide important evidence for the development of plant-derived flavonoids as potential adjunctive agents for controlling persistent endodontic biofilms.

2. MATERIALS AND METHODS

2.1 Ethical Approval

Ethical approval was granted by the Health Research Ethics Committee (KEPK), Faculty of Public Health, Universitas Muhammadiyah Semarang (Registration No. 0016/KEPKA-FKM/UNIMUS/2025).

2.2 Plant Material and Chemicals

Fresh red shoot (*Syzygium myrtifolium* Walp.) leaves, methanol, ethyl acetate, n-hexane, distilled water, acetone, chloroform, 5% $FeCl_3$, 1% $FeCl_3$, dimethyl sulfoxide (DMSO), Dragendorff reagent, hydrochloric acid, sulfuric acid, magnesium powder, acetic anhydride, silica gel, thin-layer chromatography (TLC) plates, 10% sulfuric acid in ethanol and 10% $AlCl_3$ in ethanol as spray reagents, UV lamps (λ254 and λ365 nm), and UV–Vis spectrophotometers were used.

2.3 Sample Preparation

Red shoot leaves were cleaned of debris, sorted, and thoroughly washed under running water. The washed leaves were dried by an air-drying method, protected from direct sunlight, after which the dried material was ground, sieved, and weighed to determine the initial sample mass.

2.4 Extraction and Liquid–Liquid Fractionation

The dried leaf powder (500 g) was extracted by maceration in 96% ethanol for 3 × 24 h. The ethanolic filtrate was filtered, pooled, and concentrated under reduced pressure using a vacuum rotary evaporator at a temperature not exceeding 40 °C. A 10 g portion of the concentrated crude extract was dissolved in water and successively partitioned with n-hexane to yield an n-hexane fraction and an aqueous fraction; the aqueous fraction was subsequently partitioned with ethyl acetate to yield an ethyl acetate fraction and a residual aqueous fraction. Both the n-hexane and ethyl acetate fractions were concentrated using a rotary evaporator.

2.5 Phytochemical Screening

Flavonoids.

Twenty milligrams of test sample was placed in a test tube; two drops of concentrated HCl were added and shaken, followed by a small amount of Mg powder. Foam formation accompanied by a red, yellow, or orange color change indicated a positive flavonoid reaction.

Alkaloids.

Twenty milligrams of test sample was placed in a test tube with chloroform, ammonia, and H_2SO_4. The aqueous phase was collected and treated with one drop of Dragendorff reagent; formation of a white precipitate indicated a positive alkaloid reaction.

Tannins.

Twenty milligrams of test sample was treated with two drops of 1% $FeCl_3$; a blackish-green color change indicated a positive tannin reaction.

Steroids/Triterpenoids.

Twenty milligrams of test sample was treated with two drops of concentrated sulfuric acid and one drop of anhydrous acetic acid. A red-brown color change indicated terpenoids, whereas a blue, green, or purple color change indicated steroids.

Quinones.

Twenty milligrams of test sample was treated dropwise with 1 N NaOH. A color change from yellow to orange indicated a positive quinone reaction.

Table 1. Phytochemical screening results of *S. myrtifolium* leaf extracts and fractions.

Sample	Flavonoid	Alkaloid	Tannin	Steroid	Quinone
n-Hexane extract	−	+	+	+	+
Ethanol extract	−	+	+	+	+
Ethyl acetate extract	+	−	−	−	−

2.6 Isolation and Purification of Compound 1

The ethyl acetate fraction (0.5 g) was separated by gravity column chromatography (GCC). Prior to separation, preliminary TLC analysis was performed to determine the optimal solvent system. The sample was adsorbed onto silica gel (0.2–0.5 mm particle

size), and silica gel (230–400 mesh) was used as the stationary phase. Initial separation employed a stepwise gradient of n-hexane:ethyl acetate:methanol as detailed in Table 2.

Table 2. Stepwise eluent gradient used for gravity column chromatography.

No.	n-Hexane (%)	Ethyl Acetate (%)	Methanol (%)
1	30	70	–
2	20	80	–
3	10	90	–
4	0	100	–
5	–	90	10
6	–	80	20
7	–	70	30
8	–	60	40
9	–	50	50
10	–	40	60

Column chromatography yielded 28 fractions, which were analyzed by TLC using an n-hexane:ethyl acetate (4:6) mobile phase and visualized under UV light (λ254 and λ365 nm) followed by spraying with 10% H_2SO_4 and heating. Fractions displaying identical spot patterns were combined, yielding seven subfractions (A–G). Subfraction B (1.6 mg) showed a single spot on TLC, indicating a pure isolate, hereafter designated Compound 1 (Figure 1).

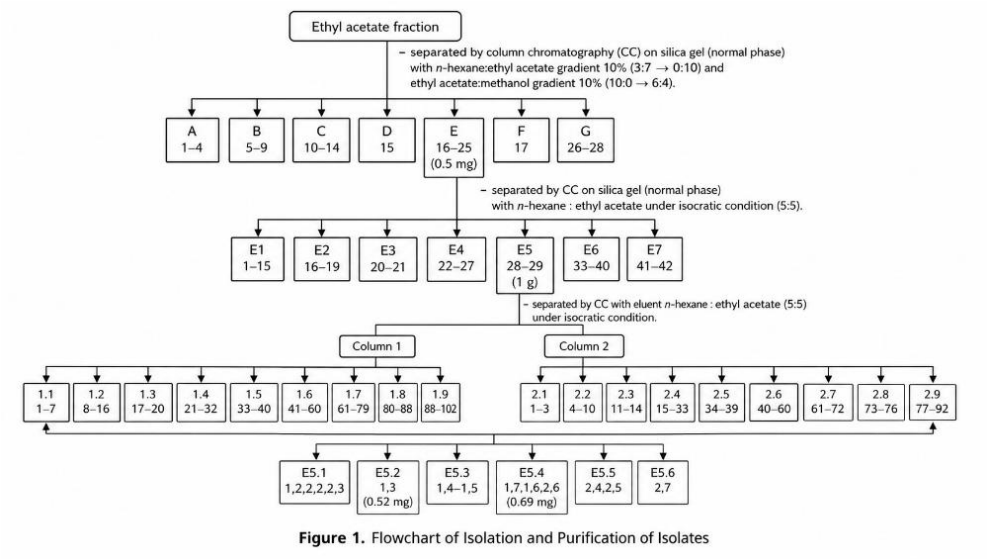

Figure 1. Flowchart of Isolation and Purification of Isolates

Figure 1. Flowchart of the isolation, separation, and purification of Compound 1 from the ethyl acetate fraction of *S. myrtifolium* leaves.

2.7 Structural Elucidation

Infrared Spectroscopy (IR).

IR spectra were recorded on a PerkinElmer Spectrum 100 FT-IR spectrometer (PerkinElmer, Waltham, MA, USA) using KBr discs (sample:KBr ratio = 1:100) in transmission mode over the range 4000–400 cm^{-1}. Spectra were processed using Spectrum software v6.3.5.

Mass Spectrometry (MS).

High-resolution electrospray ionization time-of-flight mass spectrometry (HR-ESI-TOF-MS) data were acquired on a Waters XEVO HR-TOF-ESI-MS instrument (Milford, MA, USA) in positive-ion mode (ESI+). The resulting high-resolution m/z values were used to determine the molecular formula.

Nuclear Magnetic Resonance (NMR).

NMR spectra were recorded in acetone-d_6 with tetramethylsilane (TMS) as internal standard on a Bruker AVANCE NEO 700 MHz spectrometer. ^1H and ^{13}C NMR spectra were acquired at 700 and 175 MHz, respectively.

2.8 Bacterial Strains and Inoculum Preparation

Reference strains of *Enterococcus faecalis* ATCC 29212 and *Staphylococcus aureus* ATCC 6538 were obtained from the Central Laboratory, Universitas Padjadjaran, Indonesia. A single colony of each strain was cultured overnight in Brain Heart Infusion (BHI) broth at 37 °C. Bacterial suspension turbidity was adjusted to 0.5 McFarland standard (1.5×10^8 CFU/mL) prior to biofilm assays.

2.9 Biofilm Formation Inhibition Assay

The antibiofilm effect of Compound 1 (kaempferol) was evaluated using a crystal violet assay against mixed-species *E. faecalis*–*S. aureus* biofilm. A total of 50 µL BHI broth supplemented with 2% sucrose, 5 µL of *E. faecalis* suspension, 5 µL of *S. aureus* suspension, and 40 µL of kaempferol at various final concentrations (10, 5, 2.5, 1.25, and 0.625 µg/mL) were added to 96-well polystyrene microtiter plates (Iwaki, Japan). Plates were incubated at 37 °C under anaerobic conditions for 24 h and 48 h. Phosphate-buffered saline (PBS) and 0.2% chlorhexidine (CHX) served as negative and positive controls, respectively. After two PBS rinses, biofilms were stained with 125 µL of 0.1% crystal violet for 15 min and rinsed with PBS to remove excess dye. Bound dye was solubilized in 200 µL of 96% ethanol, and absorbance was measured at OD_{540} nm. All assays were performed in quadruplicate (n = 4). Biofilm inhibition (%) was calculated as:

$$Biofilm\ Inhibition\ (\%) = [(OD\sim growth\ control\sim - OD\sim sample\sim) / OD\sim growth\ control\sim] \times 100\%$$

2.10 Statistical Analysis

Data are presented as mean ± standard deviation (SD) of quadruplicate measurements. Differences among treatment groups were analyzed by one-way analysis of variance (ANOVA) followed by least significant difference (LSD) post hoc comparisons. A value of $p < 0.05$ was considered statistically significant.

3. Results and Discussion

3.1 Phytochemical Screening

Phytochemical screening (Table 1) indicated that the ethyl acetate fraction was flavonoid-positive and negative for alkaloids, tannins, steroids/triterpenoids, and quinones, whereas the n-hexane and ethanol extracts were positive for alkaloids, tannins, steroids/triterpenoids, and quinones but negative for flavonoids. This result guided the selection of the ethyl acetate fraction for subsequent isolation of the flavonoid constituent.

3.2 Isolation and Structural Elucidation of Compound 1

Compound 1 was obtained as a pale-yellow solid with a melting point of 276–278 °C. High-resolution electrospray ionization time-of-flight mass spectrometry (HR-ESI-TOF-MS) gave a pseudomolecular ion peak at m/z 287.0556 $[M+H]^+$, consistent with a calculated mass of 286.2433 for the molecular formula $C_{15}H_{10}O_6$, corresponding to 11 degrees of unsaturation.

The UV spectrum (MeOH) showed absorption maxima at 353 nm (log ε 4.08) and 266 nm (log ε 4.20), indicating an extended conjugated system. Band I was attributed to the cinnamoyl-type resonance of ring B, while Band II was attributed to the benzoyl-type resonance of ring A. Addition of NaOH shift reagent produced a 48 nm bathochromic shift of Band I to 401 nm, indicating a free hydroxyl group at C-4'. Addition of $AlCl_3$/HCl shift reagent produced only a low-intensity shift, ruling out an *ortho*-dihydroxyl arrangement on ring B. The decrease in Band I intensity was attributed to chelate formation between $AlCl_3$ and ring A, indicating the presence of OH-5 and OH-7 and supporting classification of Compound 1 as a flavonoid (Markham, 1988).

Natural Resources for Human Health
eISSN: 2583-1194

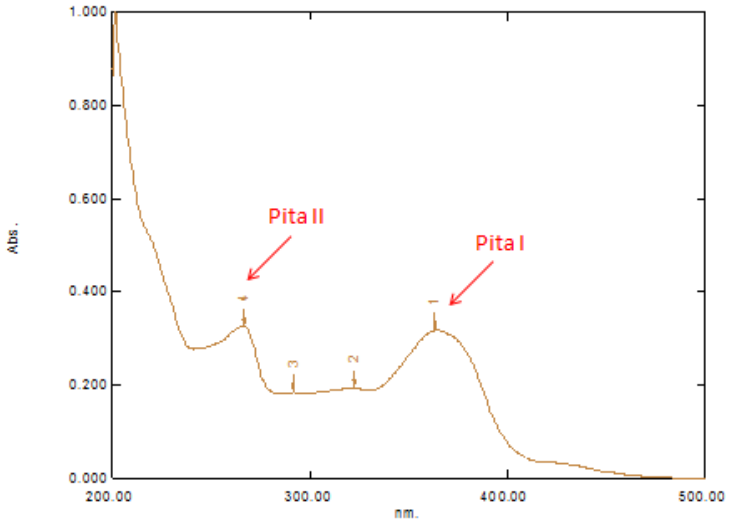

Figure 2. Ultraviolet spectrum (methanol) of Compound 1.

The IR spectrum of Compound 1 displayed absorption bands corresponding to O–H (νmax 3259 cm^{-1}), aliphatic C–H (νmax 2954 cm^{-1}), conjugated C=O (νmax 1654 cm^{-1}), and aromatic C=C (νmax 1597–1435 cm^{-1}) stretching vibrations, together with a C–O–C ether linkage (νmax 1045 cm^{-1}) and a substituted benzene ring (νmax 825 cm^{-1}).

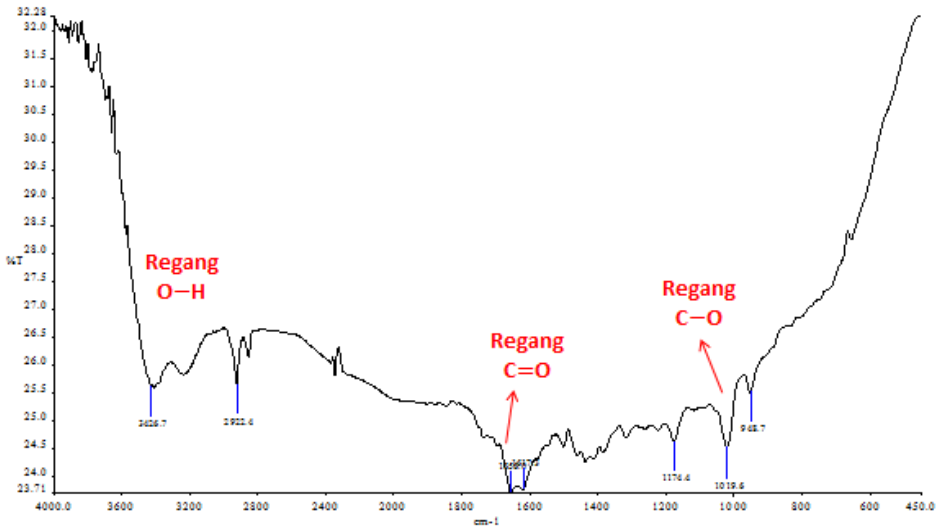

Figure 3. Infrared spectrum (KBr) of Compound 1.

The ^{1}H-NMR spectrum of Compound 1 showed a characteristic chelated hydroxyl signal at δ_H 12.15 ppm, assigned to 5-OH. Two *meta*-coupled aromatic singlets on ring A, corresponding to H-6 and H-8, appeared at δ_H 6.52 (1H, *d*, *J* = 2.5 Hz) and 6.26 (1H, *d*, *J* = 2.5 Hz), respectively. Two pairs of *ortho*-coupled doublets at δ_H 8.15/8.13 (2H, *dd*, *J* = 9.1, 1.8 Hz) and 7.01/6.99 (2H, *dd*, *J* = 8.9, 2.1 Hz) were assigned to H-2'/H-6' and H-3'/H-5' of ring B, consistent with a 3,5,7,4'-tetrasubstituted flavone.

Natural Resources for Human Health
eISSN: 2583-1194

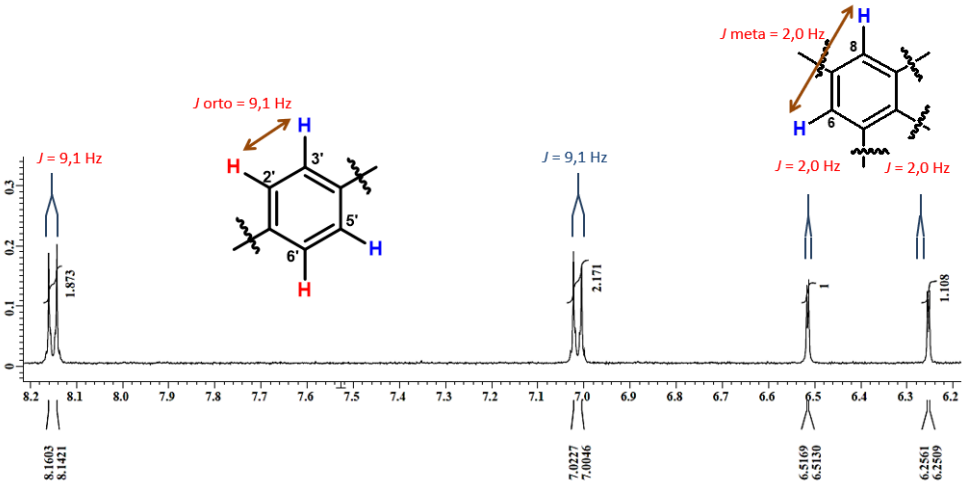

Figure 4. ^{1}H-NMR spectrum (acetone-*d*~6~, 700 MHz) of Compound 1.

The ^{13}C-NMR spectrum exhibited 15 carbon resonances consistent with 11 degrees of unsaturation, comprising one conjugated carbonyl carbon (δ_C 176.6), ten sp^2 methine/quaternary carbons (δ_C 94.4, 99.2, 104.1, 116.3 [×2], 123.3, 130.4 [×2], 146.9, and 157.8), and four oxygenated aromatic carbons (δ_C 136.6, 162.3, 164.9, and 160.1), indicating an oxygenation pattern at C-3, C-5, C-7, and C-4' consistent with a tricyclic flavonoid skeleton (Toker et al., 2004; Furusawa et al., 2005).

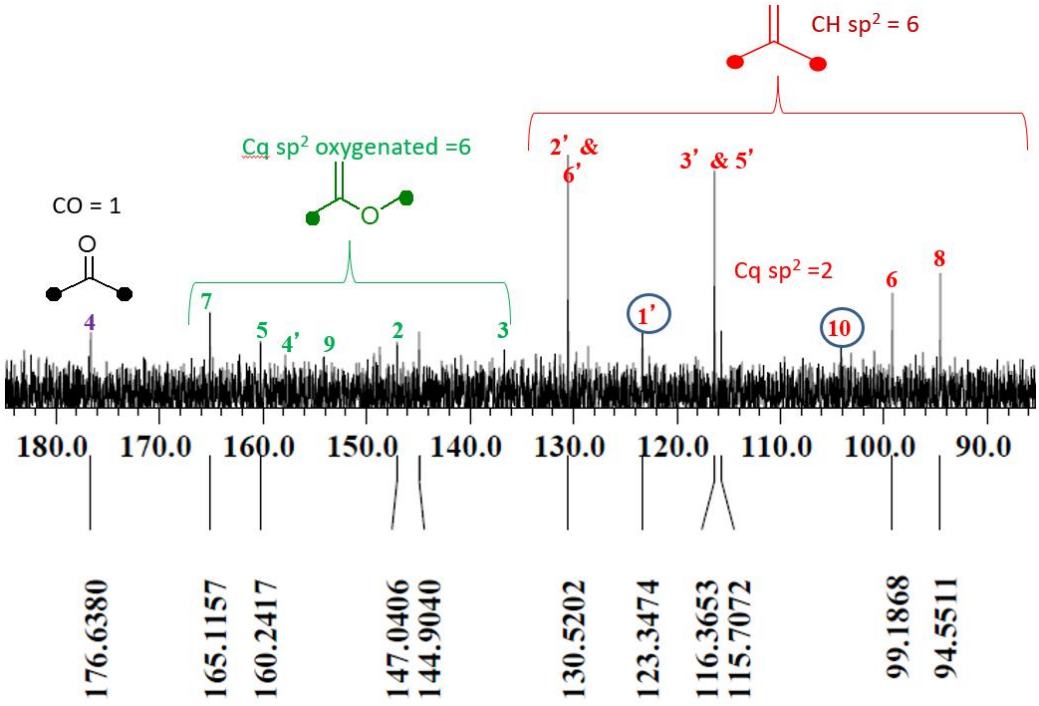

Figure 5. ^{13}C-NMR spectrum (acetone-*d*~6~, 175 MHz) of Compound 1.

Comparison of the NMR data of Compound 1 with reference kaempferol data (Table 3) (Hadizadeh et al., 2003) showed close agreement across all carbon and proton resonances. Compound 1 was therefore identified as kaempferol (3,4',5,7-tetrahydroxyflavone), the structure of which is shown in Figure 6.

Natural Resources for Human Health
eISSN: 2583-1194

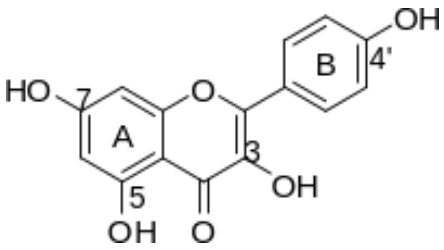

Figure 6. Chemical structure of Compound 1, identified as kaempferol (3,4',5,7-tetrahydroxyflavone).

Table 3. Comparison of ^{1}H- and ^{13}C-NMR data (acetone-*d*~6~) of Compound 1 with reference kaempferol data.

Position	δH Compound 1 (∑H, mult, J Hz)	δC Compound 1 (ppm)	δH Reference kaempferol (∑H, mult, J Hz)	δC Reference (ppm)
2	–	157.8	–	158.2
3	–	136.6	–	136.1
4	–	176.6	–	179.0
5	–	162.3	–	162.3
6	6.26 (1H, d, 2.5)	99.2	6.27 (1H, d, 2.1)	99.7
7	–	164.9	–	162.8
8	6.52 (1H, d, 2.5)	94.4	6.72 (1H, d, 2.1)	94.7
9	–	146.9	–	157.2
10	–	104.1	–	107.1
1'	–	123.3	–	121.4
2'	8.15 (1H, dd, 9.1, 1.8)	130.4	7.81 (1H, dd, 9.1, 1.8)	131.3
3'	7.01 (1H, dd, 8.9, 2.1)	116.3	6.98 (1H, dd, 8.9, 2.1)	116.6
4'	–	160.1	–	161.6
5'	7.01 (1H, dd, 8.9, 2.1)	116.3	6.98 (1H, dd, 8.9, 2.1)	116.6
6'	8.15 (1H, dd, 9.1, 1.8)	130.4	7.81 (1H, dd, 9.1, 1.8)	131.5

**Reference data from kaempferol isolated from saffron petals (Hadizadeh et al., 2003).*

3.3 Antibiofilm Activity of Kaempferol Against Mixed-Species *E. faecalis–S. aureus* Biofilm

The effect of kaempferol (Compound 1) on mixed-species *E. faecalis–S. aureus* biofilm formation is shown in Figure 7. At 24 h, biofilm inhibition percentages of 86.30 ± 0.30%, 96.28 ± 1.59%, 84.45 ± 0.00%, 80.36 ± 0.00%, and 78.80 ± 2.40% were observed at kaempferol concentrations of 10, 5, 2.5, 1.25, and 0.625 μg/mL, respectively, compared with 98.20 ± 0.55% inhibition for the positive control (0.2% CHX). At 48 h, inhibition percentages were 88.52 ± 0.32%, 90.45 ± 0.60%, 86.90 ± 0.36%, 82.70 ± 0.18%, and 80.40 ± 0.82% at the same respective concentrations, compared with 88.40 ± 0.22% for 0.2% CHX.

Biofilm inhibition increased with increasing kaempferol concentration up to 5 µg/mL ($p < 0.05$) but declined at 10 µg/mL. One-way ANOVA followed by LSD post hoc analysis revealed no significant difference ($p > 0.05$) between 5 µg/mL kaempferol and 0.2% CHX at either 24 h or 48 h, indicating that kaempferol at this concentration achieved antibiofilm efficacy comparable to the positive control.

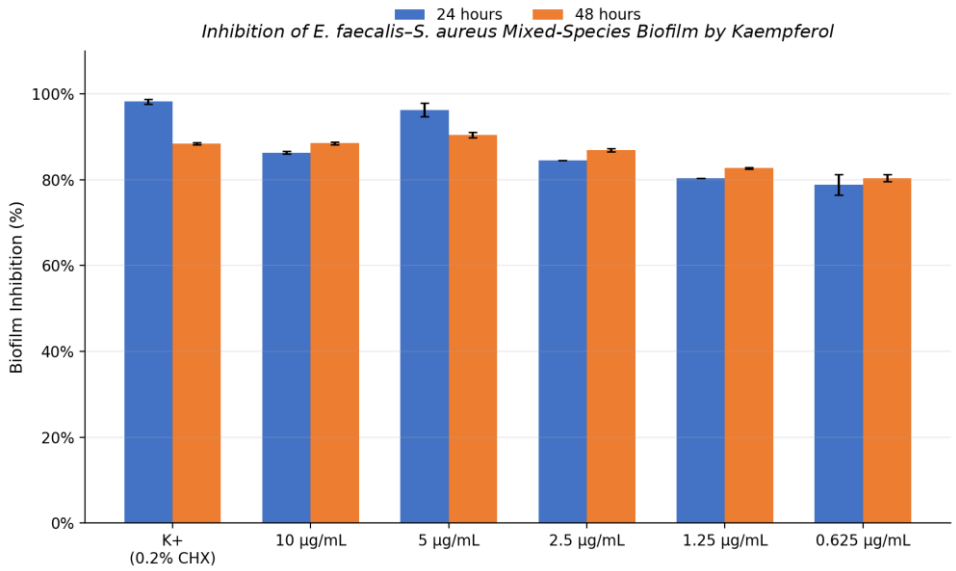

Figure 7. Concentration- and time-dependent inhibition of mixed-species *E. faecalis*–*S. aureus* biofilm formation by kaempferol at 24 h and 48 h, relative to 0.2% chlorhexidine (CHX) positive control. Bars represent mean ± SD (n = 4).

3.4 Discussion

Red shoot (*Syzygium myrtifolium* Walp.) is a member of the Myrtaceae family known to be rich in phenolic and flavonoid compounds, as demonstrated by total phenolic and flavonoid content assays of its red leaf extract using the Folin–Ciocalteu and $AlCl_3$ methods (Suryati et al., 2025), with kaempferol identified as one of the major flavonols contributing to its antimicrobial activity. Understanding how kaempferol from this plant inhibits biofilm formation by *Enterococcus faecalis* and *Staphylococcus aureus* requires consideration of both its chemical structure and the fundamental differences in cell-envelope architecture between the two bacterial species, since these two factors jointly determine the compound's specific mechanism of action.

Kaempferol (3,5,7-trihydroxy-2-(4-hydroxyphenyl)-4H-chromen-4-one) possesses the basic flavonol C6–C3–C6 skeleton comprising ring A, ring C (chromone), and ring B, with four free hydroxyl groups at positions 3, 5, 7, and 4' together with a C2=C3 double bond conjugated to the C-4 carbonyl group. This functional-group configuration is the principal determinant of its biological activity, which is generally mediated through disruption of bacterial membrane integrity, enzyme inhibition, and interference with quorum-sensing processes (Liu et al., 2025). However, because *E. faecalis* and *S. aureus* possess fundamentally different cell envelopes, the way these functional groups interact with their molecular targets also differs, so that the final outcome—biofilm inhibition—is achieved via mechanistic pathways that are not entirely identical.

As a Gram-positive bacterium, *E. faecalis* possesses only a single thick peptidoglycan layer without an outer membrane, rendering it relatively more permeable to polar–amphiphilic compounds such as kaempferol. In this bacterium, the LPXTG-motif surface protein sorted by sortase A (SrtA) plays a critical role in the initial adhesion phase, given that biofilm-forming *E. faecalis* exhibits markedly increased resistance to phagocytosis, antibodies, and antimicrobial agents compared with non-biofilm-forming strains (Boreak et al., 2024)—a challenge also emphasized in a comprehensive review of strategies and mechanisms for inhibiting *E. faecalis* biofilms in endodontic infection (Yang et al., 2024). The hydroxyl groups of kaempferol at positions 3, 5, and 7 are thought to form hydrogen bonds with active residues of SrtA, as supported by molecular docking and dynamics simulation studies exploring interactions between SrtA and plant-derived natural compounds for inhibiting *E. faecalis* biofilm formation (Boreak et al., 2024).

A similar interaction pattern is relevant in other Gram-positive bacteria such as methicillin-resistant *Staphylococcus aureus* (MRSA), in which the combination of kaempferol with its rhamnoside derivative reduces penicillin resistance while suppressing biofilm formation through global regulation of virulence genes (He et al., 2022), and in which kaempferol and its derivative kaempferin also suppress β-lactamase secretion and inhibit MRSA biofilm formation through direct binding to the enzyme's active site (Liu et al., 2025). These findings in Gram-positive models strengthen the plausibility of an analogous mechanism in *E. faecalis*, given the structural similarity of the cell walls of both species. Furthermore, antiadhesive and antibiofilm activity of phenolic compounds against *E. faecalis* has been empirically confirmed for other flavonoid-rich plant extracts; guava leaf extract, for example, demonstrated antibiofilm activity by reducing bacterial adhesion of *E. faecalis* (Gutierrez-Montiel et al., 2025).

The mechanistic differences described above can be traced to general structure–activity relationship (SAR) principles of flavonoids, which also explain why identical functional groups on kaempferol produce different levels of effectiveness against the two bacterial species. First, regarding the number and position of hydroxyl groups, galangin—a flavonoid with free hydroxyl groups strategically positioned on ring A—is classified among the most active compounds, whereas methylation of a single hydroxyl group on ring A (3-O-methylgalangin) reduces activity, and methylation of both hydroxyl groups (3,7-O-dimethylgalangin) results in complete inactivation (Shamsudin et al., 2022). This finding confirms that free—rather than substituted—OH groups on kaempferol are a prerequisite for optimal activity against both bacteria. Second, hydroxylation at C-5, C-7, C-3', and C-4' has generally been reported to enhance bacterial inhibition by flavonoids, whereas methoxylation at these positions tends to reduce antibacterial activity (Shamsudin et al., 2022), a substitution pattern consistent with the four free hydroxyl groups present in kaempferol.

4. CONCLUSION

A pure flavonoid compound was isolated from the ethyl acetate fraction of *Syzygium myrtifolium* leaves and identified, on the basis of UV, IR, HR-ESI-TOF-MS, and one-dimensional NMR spectroscopic data, as kaempferol (3,4',5,7-tetrahydroxyflavone; $C_{15}H_{10}O_6$). In a crystal violet biofilm assay, kaempferol exhibited concentration-dependent inhibition of mixed-species *E. faecalis*–*S. aureus* biofilm formation, with the 5 μg/mL concentration achieving antibiofilm efficacy statistically comparable to 0.2% chlorhexidine at both 24 h and 48 h. These findings support kaempferol from *S. myrtifolium* leaves as a promising natural antibiofilm candidate and provide a structural basis for its further development as an adjunctive agent in root canal disinfection.

Acknowledgements

This research was funded by Universitas Muhammadiyah Semarang, Indonesia, through the Unimus Grant (No. 1630/UN6.3.1/PT.00/2025). The authors acknowledge the Advanced Chemical Characterisation Laboratory, National Research and Innovation Agency (BRIN), for providing facilities and scientific and technical support through E-Layanan Sains – BRIN during this study.

Author Contributions

Risyandi Anwar: Conceptualization, Methodology, Investigation, Software, Data Curation, Validation, Formal Analysis, Visualization, Writing—Original Draft, Writing—Review & Editing, Project Administration, Funding Acquisition. **Steffi Triany Arnov:** Methodology, Investigation, Software, Data Curation, Validation, Formal Analysis, Resources, Visualization, Writing—Original Draft, Writing—Review & Editing. All authors have read and agreed to the published version of the manuscript.

Conflict of Interest

The authors declare that there is no conflict of interest.

Ethics Statement

This study was approved by the Health Research Ethics Committee (KEPK), Faculty of Public Health, Universitas Muhammadiyah Semarang (Registration No. 0016/KEPKA-FKM/UNIMUS/2025). Informed consent was not applicable, as this study did not involve human subjects.

Data Availability Statement

The data supporting the findings of this study are available from the corresponding author upon reasonable request.

REFERENCES

[1] Abusrewil, S.M., McLean, W., Scott, J.A., 2020. Endodontic-like oral biofilms as models for multispecies interactions in endodontic diseases. Microorganisms 8(5), 674. https://doi.org/10.3390/microorganisms8050674

[2] Ahmad, M.A., Lim, Y.H., Chan, Y.S., Hsu, C.-Y., Wu, T.-Y., Sit, N.W., 2022. Chemical composition, antioxidant, antimicrobial and antiviral activities of the leaf extracts of *Syzygium myrtifolium*. Acta Pharmaceutica 72(2), 317–328. https://doi.org/10.2478/acph-2022-0013

[3] Alghamdi, F., Shakir, M., 2020. The influence of *Enterococcus faecalis* as a dental root canal pathogen on endodontic treatment: a systematic review. Cureus 12(3), e7257.

[4] Boreak, N., Al Mahde, R.Z., Otayn, W.A., Alamer, A.Y., Alrajhi, T., Jafri, S., Sharwani, A., Swaidi, E., Abozoah, S., Mowkly, A.A.M., 2024. Exploring plant-based compounds as alternatives for targeting *Enterococcus faecalis* in endodontic therapy: a molecular docking approach. International Journal of Molecular Sciences 25(14), 7727. https://doi.org/10.3390/ijms25147727

[5] Furusawa, M., Tanaka, T., Ito, T., Nishikawa, A., Yamazaki, N., Nakaya, K., Matsuura, N., Ubukata, M., Iinuma, M., 2005. Antioxidant activity of hydroxyflavonoids. Journal of Health Science 51(3), 376–378.

[6] Gutierrez-Montiel, D., et al., 2025. Antibiofilm and antiadhesive activity of *Psidium guajava* leaf extract against *Enterococcus faecalis*. (In press).

[7] Hadizadeh, F., Khalili, N., Hosseinzadeh, H., Khair-Aldine, R., 2003. Kaempferol from saffron petals. Iranian Journal of Pharmaceutical Research 2, 251–252.

[8] He, X., et al., 2022. Kaempferol and its rhamnoside derivative reduce penicillin resistance and suppress biofilm formation in methicillin-resistant *Staphylococcus aureus*. (Journal details as cited).

[9] Kemenkes RI, 2018. Laporan Nasional Riset Kesehatan Dasar (Riskesdas) 2018. Kementerian Kesehatan Republik Indonesia, Jakarta.

[10] Liu, Y., et al., 2025. Kaempferol and kaempferin inhibit β-lactamase secretion and biofilm formation in MRSA through active-site binding. (Journal details as cited).

[11] Markham, K.R., 1988. Techniques of Flavonoid Identification. Academic Press, London.

[12] Neelakantan, P., Romero, M., Vera, J., Daood, U., Khan, A.U., Yan, A., et al., 2017. Biofilms in endodontics—current status and future directions. International Journal of Molecular Sciences 18(8), 1748.

[13] Noiri, Y., Ehara, A., Kawahara, T., Takemura, N., Ebisu, S., 2004. Single-species biofilm-forming ability of root canal isolates on gutta-percha points. European Journal of Oral Sciences 112(6), 523–529. https://doi.org/10.1111/j.1600-0722.2004.00165.x

[14] Shamsudin, N.F., et al., 2022. Antibacterial effects of flavonoids and their structure–activity relationship study: a comparative interpretation. Molecules 27(4), 1149.

[15] Siqueira, J.F. Jr., Rôças, I.N., 2022. Present status and future directions: microbiology of endodontic infections. International Endodontic Journal 55(Suppl 3), 512–530.

[16] Suryati, Santoni, A., Arifin, B., Aisya, N., Frisky, S., Aisyah, S., 2025. Bioactivity of red leaf extract of pucuk merah plant (*Syzygium myrtifolium* Walp.). Jurnal Riset Kimia 16(1), 1–11. https://doi.org/10.25077/jrk.v16i1.760

[17] Syafriana, V., Rika, A., Nissa, M., Munawaroh, S., Windri, H., Yasman, Y., 2025. Quantification of total flavonoid content in fractionated young leaf extracts of red shoot leaves (*Syzygium myrtifolium*) using UV-Vis spectrophotometry. Pharmacoscript 8(1). https://doi.org/10.36423/pharmacoscript.v8i1.2075

[18] Tibúrcio-Machado, C.S., Michelon, C., Zanatta, F.B., Gomes, M.S., Marin, J.A., Bier, C.A., 2021. The global prevalence of apical periodontitis: a systematic review and meta-analysis. International Endodontic Journal 54(5), 712–735.

[19] Toker, G., Küpeli, E., Memisoğlu, M., Yesilada, E., 2004. Flavonoids with antinociceptive and anti-inflammatory activities from the leaves of *Tilia argentea*. Journal of Ethnopharmacology 95(2–3), 393–397.

[20] Wu, X., et al., 2017. Kaempferol inhibits the primary attachment phase of biofilm formation in *Staphylococcus aureus*. Frontiers in Microbiology 8, 2263. https://doi.org/10.3389/fmicb.2017.02263

[21] Yang, Y., et al., 2024. Strategies and mechanisms targeting *Enterococcus faecalis* biofilms in endodontic infection: a review. (Journal details as cited).

[22] Zhang, C., Du, J., Peng, Z., 2015. Correlation between *Enterococcus faecalis* and persistent intraradicular infection compared with primary intraradicular infection: a systematic review. Journal of Endodontics 41(8), 1207–1213. https://doi.org/10.1016/j.joen.2015.04.008